Substrate-Dependent Inhibition of Organic Anion Transporting Polypeptide 1B1: Comparative Analysis with Prototypical Probe Substrates, Estradiol-17β-Glucuronide, Estrone-3-Sulfate, and Sulfobromophthalein

Saki Izumi, Yoshitane Nozaki, Takafumi Komori, Kazuya Maeda, Osamu Takenaka, Kazutomi Kusano, Tsutomu Yoshimura, Hiroyuki Kusuhara, and Yuichi Sugiyama

Drug Metabolism and Pharmacokinetics Japan, Tsukuba Research Laboratories, Eisai Co. Ltd., 5-1-3 Tokodai, Tsukuba-shi, Ibaraki, 300-2635, Japan (S. I., Y. N., T. K., O. T., K. K., T. Y.)

Laboratory of Molecular Pharmacokinetics, Graduate School of Pharmaceutical Sciences, The University of Tokyo, 7-3-1 Hongo, Bunkyo-ku, Tokyo 113-0033, Japan (K. M., H. K.)

Sugiyama Laboratory, RIKEN Innovation Center, Research Cluster for Innovation, RIKEN, 1-6 Suehiro-cho, Tsurumi-ku, Yokohama-shi, Kanagawa 230-0045, Japan (Y. S.)

1

Running Title Page

Running title: Substrate-Dependent Inhibition of OATP1B1

Corresponding Author: Yuichi Sugiyama, Ph. D.

Address: Sugiyama Laboratory, RIKEN Innovation Center, RIKEN Research Cluster for Innovation, RIKEN, 1-6 Suehiro-cho, Tsurumi-ku, Yokohama-shi, Kanagawa 230-0045, Japan

Phone: +81-45-506-1814

FAX: +81-45-506-1800

e-mail: ychi.sugiyama@riken.jp

Number of text pages: 30

Number of tables: 2

Number of figures: 4

Number of supplemental figure: 1

Number of supplemental tables: 3

Number of references: 39

Number of words in the Abstract: 244

Number of words in the Introduction: 741

Number of words in the Discussion: 1483

Abbreviations:

BSP, sulfobromophthalein; CsA, cyclosporin A; CYP, cytochrome P450; DDI, drug-drug interaction; DMSO, dimethylsulfoxide; E_2G, estradiol-17β-glucuronide; E_1S, estrone-3-sulfate; EMA, European Medicines Agency; FDA, Food and Drug Administration; ITC, International Transporter Consortium; OATP, organic anion transporting polypeptide; PBPK, physiologically

based pharmacokinetic; statin, 3-hydroxymethylglutaryl-CoA reductase inhibitor; TCA,

taurocholate.

Abstract

Organic anion transporting polypeptide (OATP) 1B1 plays an important role in the hepatic uptake of many drugs, and the evaluation of OATP1B1-mediated drug-drug interactions (DDIs) is emphasized in the latest DDI (draft) guidance from US and EU regulatory agencies. It has been suggested that some OATP1B1 inhibitors show a discrepancy in their inhibitory potential depending on the substrates used in the cell-based assay. In this study, inhibitory effects of fourteen compounds on the OATP1B1-mediated uptake of prototypical substrates, [^{3}H]estradiol-17β-glucuronide (E$_2$G), [^{3}H]estrone-3-sulfate (E$_1$S), and [^{3}H]sulfobromophthalein (BSP) were studied in OATP1B1-transfected cells. Inhibitory potencies of tested compounds varied depending on the substrates. Ritonavir, gemfibrozil, and erythromycin caused remarkable substrate-dependent inhibition with up to 117-, 14-, and 13-fold difference in their IC$_{50}$ values, respectively. Also, clinically-relevant OATP inhibitors, rifampin and cyclosporin A exhibited up to 12- and 6-fold variation in their IC$_{50}$ values, respectively. Regardless of the inhibitors tested, the most potent OATP1B1 inhibition was observed when [^{3}H]E$_2$G was used as a substrate. Mutual inhibition studies on OATP1B1 indicated that E$_2$G and E$_1$S competitively inhibited each other, whereas BSP noncompetitively inhibited E$_2$G uptake. In addition, BSP inhibited E$_1$S in a competitive manner, but E$_1$S caused an atypical kinetics on BSP uptake. This study showed substrate-dependent inhibition of OATP1B1, and demonstrated that E$_2$G was the most sensitive in vitro OATP1B1 probe substrate among three substrates tested. This will give us an insight into the assessment of clinically relevant OATP1B1-mediated DDI in vitro with minimum potential of false-negative prediction.

4

Introduction

Pharmacokinetic drug-drug interactions (DDIs) involve altered pharmacokinetics of a drug by a concomitant medication, and consequently affect the pharmacological and/or adverse effect. As the DDIs can cause life-threatening adverse events, particularly when a therapeutic range of a substrate drug is narrow, evaluation of DDI potential of new chemical entities is an integral part during drug development from the view point of clinical safety.

During this decade, research on membrane transporters has also achieved a significant progress, and revealed a major, clinically important role of membrane transporters in the pharmacokinetics of a broad range of drugs (Mizuno et al, 2003). Along with this, inhibition of membrane transporters has been recognized as one of the underlying mechanisms of pharmacokinetic DDIs (Shitara et al., 2005). In 2010, International Transporter Consortium (ITC) published so-called "transporter white paper," where a systematic approach to transporter-mediated DDIs during drug development was proposed (Giacomini et al, 2010). Furthermore, the importance of the evaluation of transporter-mediated DDI potential of an investigational drug has been emphasized in the latest DDI draft guidance and guideline released by FDA and EMA, respectively (EMA, 2012; USFDA, 2012).

Under the circumstance, potential risk evaluation of DDI involving transporters as well as drug metabolizing enzymes at nonclinical levels has become one of the crucial tasks for scientists in pharmaceutical industries in order to prioritize and develop drug candidates with an appropriate strategy for clinical DDI studies. Two models have been proposed for quantitative prediction of transporter-mediated DDIs; a static model and a dynamic (physiologically-based pharmacokinetic, PBPK) model. The static model assumes constant concentration of inhibitors (Hirano et al., 2006; Sharma et al, 2012), whereas time-course of inhibitor concentration is considered in the PBPK model (Imamura et al., 2011; Kudo et al., 2013). The static model inevitably tends to overestimate the impact of DDIs. To overcome this, we proposed new approach to minimize false-negative prediction of transporter-mediated DDIs using the static

model (Yoshida et al., 2012a). Obviously, IC_{50} (or K_i) is a key parameter in both models. Thus, accurate estimation of IC_{50} (or K_i) for the target transporter is a crucial step to achieve the quantitative DDI prediction.

Organic Anion Transporting Polypeptide (OATP) 1B1 (*SLCO1B1*) is specifically expressed in the sinusoidal membrane of hepatocytes and mediates the hepatic uptake of a wide range of drugs, including 3-hydroxymethylglutaryl-CoA reductase inhibitors (statins), angiotensin II receptor blockers, and endothelin receptor antagonists (Abe et al., 1999; Hsiang et al., 1999; Katz et al., 2006; Yamashiro et al., 2006; van Giersbergen et al., 2007; Yamada et al., 2007; Sharma et al., 2012). It has been reported that genetic polymorphisms of OATP1B1 are associated with inter-individual variation in plasma concentration of various statins (Shitara and Sugiyama, 2006; Niemi et al., 2011) and adverse event rates of statin therapy (Link et al., 2008). Moreover, clinically relevant DDIs of OATP1B1 substrate drugs (e.g., statins) with cyclosporin A, a single dose of rifampin, and other OATP inhibitors are thought to be attributable to OATP1B1 inhibition (Shitara et al., 2003; Maeda et al., 2011; Niemi et al., 2011). These cumulative data suggest the clinical importance of OATP1B1 in the drug disposition, and consequently OATP1B1 has been recognized as an important transporter in the ITC white paper and regulatory DDI guidance and guideline (Giacomini et al., 2010; EMA, 2012; USFDA, 2012).

When evaluating inhibitory potency of compounds of interest on OATP1B1, in vitro assay with OATP1B1-transfected cells using an appropriate probe substrate has been widely conducted. Meanwhile, Noé et al. (2007) reported that inhibitory potency of gemfibrozil on OATP1B1 depends on the substrates employed in their in vitro studies. This suggests that inhibition of OATP1B1 can be over- or under-estimated depending on the substrates selected, potentially resulting in false-negative prediction of OATP1B1-mediated DDIs in the worst-case scenario. Thus, we should pay much attention to OATP1B1 probe substrate for in vitro inhibition assay as in the case of CYP3A4 (Kenworthy et al., 1999; Obach et al., 2006),

6

OATP2B1 (Shirasaka et al., 2012), and OCT2 (Zolk et al., 2009), but limited information is available on the substrate-dependent inhibition of OATP1B1.

Therefore, this study compared the inhibition profiles of fourteen compounds for OATP1B1 using prototypical OATP1B1 probe substrates, estradiol-17β-glucuronide (E_2G), estrone-3-sulfate (E_1S), and sulfobromophthalein (BSP), which have been widely used for in vitro studies. Furthermore, to provide an insight into the binding sites of the three substrates on OATP1B1, mutual inhibition studies were performed. Our results suggested the usefulness of E_2G as a most likely sensitive in vitro OATP1B1 probe substrate.

Materials and Methods

Materials

[^{3}H]Estradiol-17β-glucuronide ([^{3}H]E$_2$G, 50.3 Ci/mmol) and [^{3}H]estrone-3-sulfate ([^{3}H]E$_1$S, 54.3 Ci/mmol) were purchased from PerkinElmer Life Sciences (Boston, MA). [^{3}H]Sulfobromophthalein ([^{3}H]BSP, 5.5 Ci/mmol) was synthesized in HARTMANN ANALYTIC GmbH (Braunschweig, Germany). Unlabeled E$_2$G, E$_1$S, BSP, rifampin, taurocholate (TCA), ketoconazole, gemfibrozil, verapamil, and probenecid were purchased from Sigma-Aldrich (St. Louis, MO). Cyclosporin A (CsA), erythromycin, and cimetidine were from Wako Pure Chemical Industries, Ltd. (Osaka, Japan). Tacrolimus was purchased from LKT Laboratories Inc. (St. Paul, MN), and ritonavir was obtained from Abbot Laboratories and used with purification. All other chemicals were of analytical grade and commercially available.

Uptake and Inhibition Studies Using Transfected Cells

The OATP1B1 (*SLCO1B1*) open reading frame was cloned into the KpnI/XhoI sites of an expression vector pcDNA3.1 (Invitrogen Corporation, Carlsbad, CA), and the inserted sequence was confirmed by DNA sequencing. The expression vector with or without OATP1B1 cDNA was transfected into HEK293 cells using lipofectamin 2000 (Invitrogen Corporation) according to the manufacturer's protocol. The stably OATP1B1-transfected cells and its control cells were established and maintained in Dulbecco's Modified Eagle Medium (DMEM, Invitrogen Corporation) supplemented with 10% (v/v) of fetal bovine serum, penicillin (final concentration, 100 units/mL), streptomycin (100 µg/mL), and hygromycin B (80 µg/mL) in a humidified incubator containing 5% CO$_2$ gas. The cells were trypsinized and uniformly suspended in the desired volume of the culture medium to provide 4×10^5 cells/mL. One mL of the cell suspension was added to each well of a poly-D-lysine-coated 24-well plate (BD Biosciences, San Jose, CA), and the cells were further cultured in the incubator for 48 hours.

The transport study was carried out as described previously (Hirano et al., 2004). Cell

culture medium was replaced with pre-warmed Krebs Henseleit (KH) buffer (118 mM NaCl, 23.1 mM NaHCO$_3$, 4.83 mM KCl, 0.96 mM KH$_2$PO$_4$, 1.20 mM MgSO$_4$, 12.5 mM HEPES, 5.0 mM glucose, and 1.53 mM CaCl$_2$, pH 7.4), and the cells were pre-incubated for 5 min at 37 °C. The pre-incubation buffer was aspirated, and the uptake reaction was initiated by addition of 250 µL of a pre-warmed KH buffer containing a radiolabeled substrate with or without a test compound. For inhibition studies with CsA, BSP, ritonavir, rifampin, tacrolimus, E$_2$G, and gemfibrozil, each of the dimethylsufoxide (DMSO) original solutions was prepared, serially diluted with DMSO, and 1000-fold diluted with KH buffer containing a radiolabeled substrate (final DMSO concentration, 0.1%). KH buffer containing a radiolabeled substrate and 0.1% DMSO without any inhibitors was used as the solvent control. For E$_1$S, erythromycin, TCA, probenecid, and cimetidine, each of the compounds was directly dissolved in KH buffer containing a radiolabeled substrate and serially diluted with KH buffer containing the radiolabeled substrate. For ketoconazole and verapamil, each of the compounds was completely dissolved in KH buffer containing a radiolabeled substrate at acidic pH to prepare the original solution, which was serially diluted with KH buffer containing the radiolabeled substrate to prepare the working solutions. The pH of the working solutions was adjusted at 7.4 before the inhibition assays. KH buffer containing a radiolabeled substrate without any inhibitors was used as the control for inhibition studies with E$_1$S, erythromycin, TCA, ketoconazole, verapamil, probenecid, and cimetidine. The uptake was terminated at a designated time point by adding ice-cold KH buffer immediately after removal of the incubation buffer. The cells were washed twice with 1 mL of ice-cold KH buffer and lysed with 0.5 mL of 0.1 N NaOH over night at room temperature.

Resulting cell lysate was neutralized with 50 µL of 1N HCl. Four-hundred µL of the aliquot was mixed with 4 mL of scintillation fluid (Hionic-Fluor; Perkin Elmer Life Sciences), and the radioactivities associated with the cells and also incubation buffer were measured with a liquid scintillation counter (Tri-Carb 3100TR; Perkin Elmer Life Sciences). Remaining

neutralized cell lysate samples were used to quantify protein concentrations (BCA Protein Assay Kit; Thermo Fisher Scientific, Waltham, MA).

Determination of Kinetic Parameters

Uptake of a radiolabeled substrate was expressed as the uptake volume (µL/mg protein), which was given as the radioactivity associated with the cells (dpm/well) divided by the concentration in the incubation buffer (dpm/µL) and the protein amount (mg protein/well). OATP1B1-mediated uptake was obtained by subtracting the uptake into control cells from the uptake into OATP1B1-transfected cells.

Half maximal inhibitory concentration (IC_{50}) of an inhibitor was estimated by examining the inhibitory effect on the uptake of a radiolabelled substrate (% of control) using the following equation:

$$\text{uptake (\% of control)} = \frac{CL_i}{CL} \times 100 = \frac{P}{1 + \left(\dfrac{I}{IC_{50}}\right)} \tag{1}$$

where CL and CL_i represent the uptake clearance in the absence and presence of an inhibitor, respectively, and I (µM) is the concentration of the inhibitor. P was set as a free parameter to achieve the best in the nonlinear iterative least squares regression analysis. To the inhibitor which showed biphasic inhibition for OATP1B1, the following equation was applied:

$$\text{uptake (\% of control)} = \frac{CL_i}{CL} \times 100 = \frac{P_1}{1 + \left(\dfrac{I}{IC_{50,1}}\right)} + \frac{P_2}{1 + \left(\dfrac{I}{IC_{50,2}}\right)} \tag{2}$$

where $IC_{50,1}$ and $IC_{50,2}$ represent IC_{50} of high and low affinity components, respectively. P_1 and P_2 are parameters for high and low affinity components, and $P_1 / (P_1 + P_2)$ and $P_2 / (P_1 + P_2)$ represent contribution (%) of high and low affinity components, respectively. Substrate concentrations employed in this study were sufficiently lower than their K_m values, where IC_{50} theoretically approximates the K_i regardless of inhibition mechanisms, except in the case of

10

uncompetitive inhibition (Ito et all, 1998). However, as some tested compounds showed not only inhibition, but also stimulation of a substrate uptake, the term of IC_{50} was used throughout this study. The parameters were estimated by a nonlinear least-squares regression method using MULTI program (Yamaoka et al., 1981) and expressed as the mean ± computer-calculated SD.

Concentration dependence of the uptake of a substrate mediated by OATP1B1 was analyzed using the following Michaelis-Menten equation:

$$v = \frac{V_{max} \times S}{K_m + S} \tag{3}$$

where v, S, K_m, and V_{max} represent uptake velocity of the substrate (pmol/min/mg protein), the substrate concentration in the incubation buffer (μM), Michaelis constant (μM), and the maximum uptake rate (pmol/min/mg protein), respectively. When nonsaturable component was observed, the following equation was used for the analysis:

$$v = \frac{V_{max} \times S}{K_m + S} + P_{dif} \times S \tag{4}$$

where P_{dif} represents nonsaturable uptake clearance (μL/min/mg protein). Fitting was performed by a nonlinear least-squares regression method using MULTI program.

Statistical Analysis

The data are presented as mean ± SD. One-way analysis of variance followed by Dunnett's post hoc test was used to identify significant differences between groups where appropriate. $P < 0.05$ was considered significant.

11

Results

Uptake of Prototypical OATP1B1 Substrates by OATP1B1-Transfected Cells

Time profiles of the uptake of three prototypical OATP1B1 substrates, [^{3}H]E$_2$G, [^{3}H]E$_1$S, and [^{3}H]BSP by OATP1B1-transfected cells and control cells are shown in Fig. 1. The OATP1B1-transfected cells showed higher transport activities for all 3 substrates compared to the control cells, and the uptake of [^{3}H]E$_2$G and [^{3}H]BSP were linear over the first 10 min. Thus, incubation time of 5 min was selected for [^{3}H]E$_2$G (uptake in OATP1B1-transfected cells, mean ± SD, 112 ± 2 μL/mg protein; uptake in control cells, 1.93 ± 0.14 μL/mg protein) and [^{3}H]BSP uptake (OATP1B1, 503 ± 52 μL/mg protein; control, 113 ± 11 μL/mg protein) in the following inhibition and concentration dependent uptake studies. As shown in Fig. 1B, uptake of [^{3}H]E$_1$S reached steady state at 10 min in OATP1B1-transfected cells. The uptake of [^{3}H]E$_1$S was determined at 1 min, the practically earliest sampling point for subsequent analysis (OATP1B1, 132 ± 9 μL/mg protein; control, 3.97 ± 0.78 μL/mg protein).

Inhibitory Effects of Fourteen Compounds on the OATP1B1-Mediated Uptake of [^{3}H]E$_2$G, [^{3}H]E$_1$S, and [^{3}H]BSP

Inhibitory effects of unlabeled E$_1$S, CsA, BSP, ritonavir, rifampin, tacrolimus, erythromycin, E$_2$G, TCA, ketoconazole, gemfibrozil, verapamil, probenecid, and cimetidine on the OATP1B1-mediated uptake of [^{3}H]E$_2$G, [^{3}H]E$_1$S, and [^{3}H]BSP were investigated (Fig. 2). All tested compounds except for cimetidine inhibited uptake of [^{3}H]E$_2$G, [^{3}H]E$_1$S, and [^{3}H]BSP in a concentration dependent manner. Although almost all the inhibition curves were well fitted to the equation for monophasic inhibition (equation. 1), the inhibition of [^{3}H]BSP uptake by unlabeled E$_1$S was well described as a biphasic inhibition (equation. 2) with IC$_{50}$ values of 0.429 and 611 μM.

Several inhibitors showed a biphasic effect on OATP1B1-mediated uptake; stimulation at low concentrations followed by inhibition along with increasing inhibitor concentrations. Only

12

lower concentrations of E_1S, CsA, ritonavir, rifampin, E_2G, TCA, ketoconazole, verapamil, and probenecid caused a significant stimulation of [^{3}H]BSP uptake, while cimetidine significantly stimulated [^{3}H]BSP uptake over the concentration range from 3 to 1000 μM (Fig. 2 and Supplemental Table 3). Similarly, [^{3}H]E_2G and [^{3}H]E_1S uptake were significantly stimulated by some inhibitors at lower concentrations (Supplemental Table 1 and 2), but the extent of stimulation was less compared with [^{3}H]BSP uptake.

IC$_{50}$ values of inhibitors tested are summarized in Table 1, and comparison between IC$_{50}$ values on [^{3}H]E_2G, [^{3}H]E_1S, and [^{3}H]BSP uptake is shown in Fig. 3. As shown in Fig. 3A and 3B, the most potent inhibition was observed when [^{3}H]E_2G was used as a substrate, and the IC$_{50}$ of all inhibitors tested were lower than those for [^{3}H]E_1S and [^{3}H]BSP uptake. Inhibitory potencies on OATP1B1 varied depending on the substrates used, and ritonavir, gemfibrozil, and erythromycin showed a remarkable substrate-dependency. IC$_{50}$ values (μM) of ritonavir (0.397, 46.4, and 3.38 for [^{3}H]E_2G, [^{3}H]E_1S, and [^{3}H]BSP uptake, respectively), gemfibrozil (26.4, 381, and 173, respectively), and erythromycin (4.88, 13.4, and 63.3, respectively) showed up to 117-, 14-, and 13-fold variation depending on the substrates, respectively. Additionally, rifampin and CsA, which are frequently used as OATP inhibitors in clinical DDI studies, showed up to 12- (IC$_{50}$ [μM]: 0.585 for [^{3}H]E_2G versus 6.96 for [^{3}H]E_1S) and 6-fold (0.118 for [^{3}H]E_2G versus 0.732 for [^{3}H]E_1S) variation in the IC$_{50}$ values, respectively. Other inhibitors also showed 2- (BSP) to 9-fold (probenecid) discrepancy in the IC$_{50}$ values depending on the substrates selected, and [^{3}H]E_2G also provided the lowest IC$_{50}$ regardless of the inhibitors tested.

Mutual Inhibition on OATP1B1-mediated Uptake of Prototypical Substrates

Concentration dependence of OATP1B1-mediated uptake of [^{3}H]E_2G, [^{3}H]E_1S, and [^{3}H]BSP were investigated in the presence or absence of unlabeled E_2G, E_1S, and BSP to see the mode of inhibition between prototypical substrates tested. Representative data are given in Fig. 4 and obtained kinetic parameters are summarized in Table 2.

Uptake of [^{3}H]E$_2$G consisted of 1-saturable component, and the K$_m$ values significantly increased from 8.17 to 18.7 µM in the presence of unlabeled E$_1$S at 0.1 µM with minimal effect on V$_{max}$. In the presence of unlabeled BSP at 0.3 µM, the V$_{max}$ value significantly decreased to less than 22% of that in the absence of BSP with minimal effect on K$_m$. These results suggested that E$_1$S and BSP inhibited [^{3}H]E$_2$G uptake by OATP1B1 in competitive and noncompetitive manners, respectively.

Uptake of [^{3}H]E$_1$S showed a saturable component, and the K$_m$ (0.286 µM) significantly increased to 0.488 and 0.677 µM in the presence of unlabeled E$_2$G (10 µM) and BSP (0.3 µM), respectively, without affecting V$_{max}$. Thus, E$_2$G and BSP competitively inhibited OATP1B1-mediated uptake of [^{3}H]E$_1$S.

[^{3}H]BSP uptake via OATP1B1 also consisted of 1-saturable component with K$_m$ of 0.280 µM. Unlabeled E$_2$G (10 µM) showed a trend to increase and decrease the K$_m$ and V$_{max}$, respectively, but without statistically significant difference. Unlabeled E$_1$S at 10 µM showed an atypical inhibition profile for [^{3}H]BSP uptake, where E$_1$S significantly increased both K$_m$ and V$_{max}$ of [^{3}H]BSP uptake by 17- and 5-fold, respectively.

Discussion

It has been demonstrated that membrane transporters play significant roles in drug disposition, therapeutic efficacy, and adverse events, and clinical evidence showing importance of transporter-mediated DDIs is increasingly accumulating (Giacomini et al., 2010; Yoshida et al., 2012b). OATP1B1 is one of the major human hepatic uptake transporters, and clinically observed DDIs involving OATP1B1 have been reported (Shitara et al., 2003; Maeda et al., 2011; Niemi et al., 2011; Shitara et al., 2013). Regulatory agencies also consider OATP1B1 as one of the important transporters (EMA, 2012; USFDA, 2012). Selection of OATP1B1 probe substrate for in vitro study is an important topic to predict the DDI risk.

E_2G and E_1S are prototypical OATP1B1 probe substrates, and widely used in cellular uptake studies with OATP1B1-transfected cells and human hepatocytes (Hirano et al., 2004; Sharma et al., 2010). OATP1B1-transfected cells used in this study also showed significantly higher uptake of $[^3H]E_2G$ and $[^3H]E_1S$ compared to the control cells (Fig. 1). To investigate substrate-dependent interaction with OATP1B1, IC_{50} values of inhibitors calculated against $[^3H]E_2G$ and $[^3H]E_1S$ uptake are compared in Fig. 3A, which clearly demonstrated that the IC_{50} values of all inhibitors tested were higher for $[^3H]E_1S$ uptake compared to $[^3H]E_2G$ uptake. Notably, ritonavir, gemfibrozil, and rifampin showed 117-, 14-, and 12-fold higher IC_{50} values when $[^3H]E_1S$ was used as a substrate, respectively, and similar trend was also reported previously (Noé et al., 2007; Soars et al., 2012). Also, to a lesser extent, CsA produced 6-fold greater IC_{50} for $[^3H]E_1S$ uptake. Other inhibitors showed higher IC_{50} for $[^3H]E_1S$ uptake rather than $[^3H]E_2G$, but the difference was within 3-fold. These substrate-dependent differences in IC_{50} particularly for rifampin and CsA, which are used in clinic as OATP inhibitors, should be taken into account in accurately estimating the impact of OATP1B1-mediated DDIs.

BSP is also a typical OATP1B1 substrate (Cui et al., 2001; Kindla et al., 2011) and showed significantly higher uptake in OATP1B1-transfected cells compared to the control cells (Fig. 1). As observed in the relationship of IC_{50} values between $[^3H]E_2G$ and $[^3H]E_1S$, IC_{50}

15

values of all inhibitors for [^{3}H]BSP uptake were higher when comparing those for [^{3}H]E$_2$G (Fig. 3B). Among the inhibitors tested, erythromycin showed the most remarkable difference, and the IC$_{50}$ for [^{3}H]BSP uptake was 13-fold higher than that for [^{3}H]E$_2$G, although the difference between [^{3}H]E$_1$S and [^{3}H]E$_2$G was less than 3-fold. Similarly, BSP, ritonavir, tacrolimus, E$_2$G, ketoconazole, TCA, gemfibrozil, and probenecid also showed more than 5-fold higher IC$_{50}$ values for [^{3}H]BSP uptake compared to [^{3}H]E$_2$G.

These results clearly indicate substrate-dependent interaction with OATP1B1, and some inhibitors (ritonavir, gemfibrozil, erythromycin, and rifampin) caused more than 10-fold differences in the IC$_{50}$ values. This means OATP1B1-mediated DDI risk can be more than 10-fold underestimated if the substrate is not appropriately selected, which could result in false-negative DDI prediction and potentially serious clinical safety issue. Thus, careful attention will be needed when selecting an OATP1B1 probe substrate for in vitro inhibition assay as in the case of CYP3A4 (Kenworthy et al., 1999; Obach et al., 2006), OATP2B1 (Shirasaka et al., 2012), and OCT2 (Zolk et al., 2009). Although it would be ideal to evaluate DDI potentials for all OATP1B1 substrate-inhibitor combinations anticipated in clinical settings, this approach will not be practical in drug development processes, particularly at the early stage, where a large number of newly synthesized compounds are evaluated in a high-throughput manner. Among the substrates tested in this study, [^{3}H]E$_2$G was the OATP1B1 probe substrate that could most sensitively detect inhibitory potential on OATP1B1, because IC$_{50}$ of all inhibitors tested for [^{3}H]E$_2$G uptake were lower than those for [^{3}H]E$_1$S and [^{3}H]BSP uptake (Fig. 3). Therefore, this finding of E$_2$G as a sensitive OATP1B1 probe substrate will be helpful to achieve this goal.

Previously, Hirano et al. (2006) comprehensively evaluated the IC$_{50}$ values for [^{3}H]pitavastatin uptake via OATP1B1 and estimated the extent of in vivo DDIs using a static model. Although assay conditions were not identical, we have compared the IC$_{50}$ values reported by Hirano et al. (2006) with those for [^{3}H]E$_2$G uptake obtained in this study. This comparison clarified that IC$_{50}$ values for [^{3}H]pitavastatin uptake were within 2.5-fold of those

for $[^3H]E_2G$ uptake in this study, suggesting that E_2G and pitavastatin behave similarly in terms of their susceptibility to OATP1B1 inhibitors. Most recently, Sharma et al. (2012) reported that the extent of inhibition of $[^3H]E_2G$ by rifamycin SV, gemfibrozil, and a proprietary compound was similar to that observed for the inhibition of statins, and they suggested that E_2G could be a surrogate probe for statins when assessing OATP1B1 inhibition. These indicate that E_2G could be used not only as a sensitive substrate to mitigate the risk of false-negative DDI prediction, but also potentially as a surrogate probe for statins. In addition to statins, however, a broad range of drugs including angiotensin II receptor blockers (Yamashiro et al., 2006; Yamada et al., 2007), endothelin receptor antagonists (Katz et al., 2006; van Giersbergen et al., 2007), antidiabetics (Niemi et al., 2005; Zhang et al., 2006), and a diuretic (Vormfelde et al., 2008) are reported to be OATP1B1 substrates. Further studies will be needed to elucidate if E_2G could be a universal surrogate probe of OATP1B1 by comparing IC_{50} values between $[^3H]E_2G$ and OATP1B1 substrate drugs including statins and other classes of drugs.

Substrate-dependent interaction with OATP1B1 suggests that OATP1B1 has multiple/allosteric binding sites for the substrates. To gain an insight into the binding sites, mutual inhibition studies were performed (Fig. 4). $[^3H]E_2G$ and $[^3H]BSP$ showed monophasic uptake for OATP1B1, which was consistent with previous reports (Cui et al., 2001; Hirano et al, 2004; Sharma et al., 2010). As for $[^3H]E_1S$ uptake by OATP1B1-transfected cells, biphasic uptake was demonstrated by some groups (Tamai et al., 2001; Noé et al., 2007; Sharma et al., 2012) and monophasic uptake by others (Hirano et al., 2004), and the latter held true for this study. Although we do not have good explanation for the discrepancy, experimental conditions (e.g., cells, cell culture conditions, assay procedures) might be one of the underlying reasons. Through the mutual inhibition studies, it was elucidated that OATP1B1-mediated uptake of $[^3H]E_2G$ and $[^3H]E_1S$ competitively inhibited each other, suggesting that both substrates could share the same binding site. However, some inhibitors such as ritonavir, gemfibrozil, and rifampin showed notably different IC_{50} (i.e., affinity) for $[^3H]E_2G$ and $[^3H]E_1S$ uptake, and thus

17

it would be difficult to conclude that both substrates completely share the same binding site. Moreover, BSP noncompetitively inhibited $[^3H]E_2G$ uptake by OATP1B1, which suggests the presence of binding site different from that of $[^3H]E_2G$. We also analyzed the relationship between $[^3H]E_1S$ and $[^3H]BSP$ uptake in the same manner, and BSP competitively inhibited $[^3H]E_1S$ uptake, although E_1S showed atypical kinetics on $[^3H]BSP$ uptake, where both K_m and V_{max} of $[^3H]BSP$ uptake increased by 17- and 5-fold, respectively. These results suggest at least more than one binding site on OATP1B1, which might be an underlying mechanism of substrate-dependent inhibition of OATP1B1. Further kinetic analysis with molecular biology techniques as reported previously (Miyagawa et al., 2009) will be needed to identify each binding site of E_2G, E_1S, and BSP, and clarify a complex mutual interactions among them on OATP1B1.

In the inhibition studies, some compounds such as E_1S, ritonavir, and E_2G caused not only inhibition at higher concentrations, but also statistically significant stimulation of the substrate uptake at lower concentrations (Supplemental table 1, 2, and 3), and this behavior was more evident in $[^3H]BSP$ uptake (Fig. 2). Cimetidine was also found to significantly stimulate $[^3H]BSP$ uptake, but the stimulatory effect was sustained over the concentration range from 3 to 1000 μM (Supplemental table 3).. Although underlying mechanism of the observed stimulation remains to be clarified, the inhibitors at lower concentrations might have dominantly interacted with the allosteric site, resulting in stimulation of $[^3H]BSP$ uptake, while the inhibitors at higher concentrations except cimetidine might have not only interacted with the allosteric site, but also inhibited BSP binding site, resulting in net inhibition of $[^3H]BSP$ uptake. Sustained stimulation of OATP1B1-mediated $[^3H]BSP$ uptake by cimetidine over the concentration range from 3 to 1000 μM might be explainable in terms of the preferential affinity of cimetidine for allosteric site relative to BSP binding site. Although further studies will be needed to draw more definite conclusions, the significant stimulatory effect observed in this study and other study (Kindla et al., 2011) suggests the presence of multiple binding sites on OATP1B1.

18

In conclusion, inhibition potentials of fourteen compounds on OATP1B1 were comparatively analyzed using prototypical OATP1B1 probe substrates, E_2G, E_1S, and BSP, and OATP1B1 showed substrate-dependent inhibition. Some inhibitors showed more than 10-fold differences in the IC_{50} values depending on the substrate used in the in vitro inhibition studies. Among the three substrates tested, E_2G was the OATP1B1 probe substrate that could most sensitively detect inhibitory potential on OATP1B1. E_2G could be used as a sensitive probe substrate when evaluating OATP1B1 inhibition, which will help mitigate the risk of false-negative DDI prediction.

Acknowledgments

20

Authorship Contributions

Participated in research design: Izumi, Nozaki, Komori, Maeda, Takenaka, and Sugiyama.

Conducted experiments: Izumi.

Contributed new reagents or analytic tools: Maeda.

Performed data analysis: Izumi, Nozaki, Komori, and Maeda.

Wrote or contributed to the writing of the manuscript: Izumi, Nozaki, Komori, Maeda,

Takenaka, Kusano, Yoshimura, Kusuhara, and Sugiyama.

21

References

Abe T, Kakyo M, Tokui T, Nakagomi R, Nishio T, Nakai D, Nomura H, Unno M, Suzuki M, Naitoh T, Matsuno S, and Yawo H (1999) Identification of a novel gene family encoding human liver-specific organic anion transporter LST-1. *J Biol Chem* **274**:17159-17163

Cui Y, König J, Leier I, Buchholz U, and Keppler D (2001) Hepatic uptake of bilirubin and its conjugates by the human organic anion transporter SLC21A6. *J Biol Chem* **276**:9626-9630

EMA (2012) Guideline on the Investigation of Drug Interactions. *Committee for Human Medicinal Products (CHMP)*

Giacomini KM, Huang SM, Tweedie DJ, Benet LZ, Brouwer KL, Chu X, Dahlin A, Evers R, Fischer V, Hillgren KM, Hoffmaster KA, Ishikawa T, Keppler D, Kim RB, Lee CA, Niemi M, Polli JW, Sugiyama Y, Swaan PW, Ware JA, Wright SH, Yee SW, Zamek-Gliszczynski MJ, and Zhang L (2010) Membrane transporters in drug development. *Nat Rev Drug Discov* **9**:215-236

Hirano M, Maeda K, Shitara Y, and Sugiyama Y (2004) Contribution of OATP2 (OATP1B1) and OATP8 (OATP1B3) to the hepatic uptake of pitavastatin in humans. *J Pharmacol Exp Ther* **311**:139-46

Hirano M, Maeda K, Shitara Y, and Sugiyama Y (2006) Drug-drug interaction between pitavastatin and various drugs via OATP1B1. *Drug Metab Dispos* **34**:1229-1236

Hsiang B, Zhu Y, Wang Z, Wu Y, Sasseville V, Yang WP, and Kirchgessner TG (1999) A novel human hepatic organic anion transporting polypeptide (OATP2). Identification of a liver-specific human organic anion transporting polypeptide and identification of rat and human hydroxymethylglutaryl-CoA reductase inhibitor transporters. *J Biol Chem* **274**:37161-37168

Imamura Y, Murayama N, Okudaira N, Kurihara A, Okazaki O, Izumi T, Inoue K, Yuasa H,

Kusuhara H, and Sugiyama Y (2011) Prediction of fluoroquinolone-induced elevation in serum creatinine levels: a case of drug-endogenous substance interaction involving the inhibition of renal secretion. *Clin Pharmacol Ther* **89**:81-88

Ito K, Iwatsubo T, Kanamitsu S, Ueda K, Suzuki H, and Sugiyama Y (1998) Prediction of pharmacokinetic alterations caused by drug-drug interactions: metabolic interaction in the liver. *Pharmacol Rev* **50**:387-412

Katz DA, Carr R, Grimm DR, Xiong H, Holley-Shanks R, Mueller T, Leake B, Wang Q, Han L, Wang PG, Edeki T, Sahelijo L, Doan T, Allen A, Spear BB, and Kim RB (2006) Organic anion transporting polypeptide 1B1 activity classified by SLCO1B1 genotype influences atrasentan pharmacokinetics. *Clin Pharmacol Ther* **79**:186-196

Kenworthy KE, Bloomer JC, Clarke SE, and Houston JB (1999) CYP3A4 drug interactions: correlation of 10 in vitro probe substrates. *Br J Clin Pharmacol* **48**:716-727

Kindla J, Müller F, Mieth M, Fromm MF, and König J (2011) Influence of non-steroidal anti-inflammatory drugs on organic anion transporting polypeptide (OATP) 1B1- and OATP1B3-mediated drug transport. *Drug Metab Dispos* **39**:1047-1053

Kudo T, Hisaka A, Sugiyama Y, and Ito K (2013) Analysis of the repaglinide concentration increase produced by gemfibrozil and itraconazole based on the inhibition of the hepatic uptake transporter and metabolic enzymes. *Drug Metab Dispos* **41**:362-371

Link E, Parish S, Armitage J, Bowman L, Heath S, Matsuda F, Gut I, Lathrop M, and Collins R (2008) SLCO1B1 variants and statin-induced myopathy – a genomewide study. *N Engl J Med* **359**:789-799

Maeda K, Ikeda Y, Fujita T, Yoshida K, Azuma Y, Haruyama Y, Yamane N, Kumagai Y, and Sugiyama Y (2011) Identification of the rate-determining process in the hepatic clearance of atorvastatin in a clinical cassette microdosing study. *Clin Pharmacol Ther* **90**:575-581

Miyagawa M, Maeda K, Aoyama A, and Sugiyama Y (2009) The eighth and ninth

transmembrane domains in organic anion transporting polypeptide 1B1 affect the
transport kinetics of estrone-3-sulfate and estradiol-17beta-D-glucuronide. *J Pharmacol Exp Ther* **329**:551-557

Mizuno N, Niwa T, Yotsumoto Y, and Sugiyama Y (2003) Impact of drug transporter studies on
drug discovery and development. *Pharmacol Rev* **55**:425-461

Niemi M, Backman JT, Kajosaari LI, Leathart JB, Neuvonen M, Daly AK, Eichelbaum M,
Kivistö KT, and Neuvonen PJ (2005) Polymorphic organic anion transporting
polypeptide 1B1 is a major determinant of repaglinide pharmacokinetics. *Clin Pharmacol Ther* **77**:468-478

Niemi M, Pasanen MK, and Neuvonen PJ (2011) Organic anion transporting polypeptide 1B1: a
genetically polymorphic transporter of major importance for hepatic drug uptake.
Pharmacol Rev **63**:157-181

Noé J, Portmann R, Brun ME, and Funk C (2007) Substrate-dependent drug-drug interactions
between gemfibrozil, fluvastatin and other organic anion-transporting peptide (OATP)
substrates on OATP1B1, OATP2B1, and OATP1B3. *Drug Metab Dispos* **35**:1308-1314

Obach RS, Walsky RL, Venkatakrishnan K, Gaman EA, Houston JB, and Tremaine LM (2006)
The utility of in vitro cytochrome P450 inhibition data in the prediction of drug-drug
interactions. *J Pharmacol Exp Ther* **316**:336-348

Sharma P, Holmes VE, Elsby R, Lambert C, and Surry D (2010) Validation of cell-based
OATP1B1 assays to assess drug transport and the potential for drug-drug interaction to
support regulatory submissions. *Xenobiotica* **40**:24-37

Sharma P, Butters CJ, Smith V, Elsby R, and Surry D (2012) Prediction of the in vivo
OATP1B1-mediated drug-drug interaction potential of an investigational drug against a
range of statins. *Eur J Pharm Sci* **47**:244-55

Shirasaka Y, Mori T, Shichiri M, Nakanishi T, and Tamai I (2012) Functional pleiotropy of
organic anion transporting polypeptide OATP2B1 due to multiple binding sites. *Drug*

Metab Pharmacokinet **27**:360-364

Shitara Y, Itoh T, Sato H, Li AP, and Sugiyama Y (2003) Inhibition of transporter-mediated hepatic uptake as a mechanism for drug-drug interaction between cerivastatin and cyclosporin A. *J Pharmacol Exp Ther* **304**:610-616

Shitara Y, Sato H, and Sugiyama Y (2005) Evaluation of drug-drug interaction in the hepatobiliary and renal transport of drugs. *Annu Rev Pharmacol Toxicol* **45**:689-723

Shitara Y, Maeda K, Ikejiri K, Yoshida K, Horie T, and Sugiyama Y (2013) Clinical significance of organic anion transporting polypeptides (OATPs) in drug disposition: their roles in hepatic clearance and intestinal absorption. *Biopharm Drug Dispos* **34**:45-78

Soars MG, Barton P, Ismair M, Jupp R, and Riley RJ (2012) The development, characterization, and application of an OATP1B1 inhibition assay in drug discovery. *Drug Metab Dispos* **35**:1308-1314

Tamai I, Nozawa T, Koshida M, Nezu J, Sai Y, and Tsuji A (2001) Functional characterization of human organic anion transporting polypeptide B (OATP-B) in comparison with liver-specific OATP-C. *Pharm Res* **18**:1262-1269

USFDA (2012) Drug interaction studies – study design, data analysis, implications for dosing, and labeling recommendations. *Center for Drug Evaluation and Research (CDER)*

van Giersbergen PL, Treiber A, Schneiter R, Dietrich H, and Dingemanse J (2007) Inhibitory and inductive effects of rifampin on the pharmacokinetics of bosentan in healthy subjects. *Clin Pharmacol Ther* **81**:414-419

Vormfelde SV, Toliat MR, Schirmer M, Meineke I, Nürnberg P, and Brockmöller J (2008) The polymorphisms Asn130Asp and Val174Ala in OATP1B1 and the CYP2C9 allele *3 independently affect torsemide pharmacokinetics and pharmacodynamics. *Clin Pharmacol Ther* **83**:815-817

Yamada A, Maeda K, Kamiyama E, Sugiyama D, Kondo T, Shiroyanagi Y, Nakazawa H, Okano T, Adachi M, Schuetz JD, Adachi Y, Hu Z, Kusuhara H, and Sugiyama Y (2007)

Multiple human isoforms of drug transporters contribute to the hepatic and renal transport of olmesartan, a selective antagonist of the angiotensin II AT1-receptor. *Drug Metab Dispos* **35**:2166-2176

Yamaoka K, Tanigawara Y, Nakagawa T, and Uno T (1981) A pharmacokinetic analysis program (multi) for microcomputer. *J Pharmacobiodyn* **4**:879-885

Yamashiro W, Maeda K, Hirouchi M, Adachi Y, Hu Z, and Sugiyama Y (2006) Involvement of transporters in the hepatic uptake and biliary excretion of valsartan, a selective antagonist of the angiotensin II AT1-receptor, in humans. *Drug Metab Dispos* **34**:1247-1254

Yoshida K, Maeda K, and Sugiyama Y (2012a) Transporter-mediated drug-drug interactions involving OATP substrates: predictions based on in vitro inhibition studies. *Clin Pharmacol Ther* **91**:1053-1064

Yoshida K, Maeda K, and Sugiyama Y (2012b) Hepatic and intestinal drug transporters: prediction of pharmacokinetic effects caused by drug-drug interactions and genetic polymorphisms. *Annu Rev Pharmacol Toxicol* **53**:581-612

Zhang W, He YJ, Han CT, Liu ZQ, Li Q, Fan L, Tan ZR, Zhang WX, Yu BN, Wang D, Hu DL, and Zhou HH (2006) Effect of SLCO1B1 genetic polymorphism on the pharmacokinetics of nateglinide. *Br J Clin Pharmacol* **62**:567-572

Zolk O, Solbach TF, König J, and Fromm MF (2009) Structural determinants of inhibitor interaction with the human organic cation transporter OCT2 (SLC22A2). *Naunyn Schmiedebergs Arch Pharmacol* **379**:337-348

Legends for Figures

Fig. 1. Time profiles of the uptake of [^{3}H]E$_2$G (A), [^{3}H]E$_1$S (B), and [^{3}H]BSP (C) by OATP1B1-transfected cells and the control cells.

Uptake of [^{3}H]E$_2$G (0.1 µM), [^{3}H]E$_1$S (0.01µM), and [^{3}H]BSP (0.01 µM) by OATP1B1-transfected cells (closed circles) and the control cells (open circles) was determined over 30 minutes at 37 °C. Each point represents the mean ± SD (n = 3).

Fig.2. Inhibitory effects of 14 compounds on OATP1B1-mediated uptake of [^{3}H]E$_2$G, [^{3}H]E$_1$S, and [^{3}H]BSP.

Uptake of [^{3}H]E$_2$G (0.1 µM, closed circles), [^{3}H]E$_1$S (0.01 µM, open triangles), and [^{3}H]BSP (0.01 µM, open squares) were investigated in the presence and absence of unlabeled E$_1$S (A), CsA (B), BSP (C), ritonavir (D), rifampin (E), tacrolimus (F), erythromycin (G), E$_2$G (H), TCA (I), ketoconazole (J), gemfibrozil (K), verapamil (L), probenecid (M), and cimetidine (N). The data are shown as percent of control as described in *Materials and Methods*. Thick, thin, and dashed lines represent fitted lines for the uptake of [^{3}H]E$_2$G, [^{3}H]E$_1$S, and [^{3}H]BSP, respectively. Each point represents the mean ± SD (n = 6).

Fig. 3. Comparison of IC$_{50}$ values between [^{3}H]E$_2$G and [^{3}H]E$_1$S (A), [^{3}H]E$_2$G and [^{3}H]BSP (B), and [^{3}H]E$_1$S and [^{3}H]BSP (C).

IC$_{50}$ values are taken from Table 1, and each point represents the mean ± SD. The solid line and the dashed lines represent the line of unity and the lines of 1:10 and 10:1 correlations, respectively. 1, E$_1$S; 2, CsA; 3, BSP; 4, ritonavir; 5, rifampin; 6, tacrolimus; 7, erythromycin; 8, E$_2$G; 9, ketoconazole; 10, TCA; 11, verapamil; 12, gemfibrozil; 13, probenecid. IC$_{50}$ values of E$_1$S for [^{3}H]BSP uptake were eliminated from the panel B and C, because E$_1$S showed biphasic inhibition for [^{3}H]BSP uptake. The correlation coefficients were 0.870 (A), 0.987 (B), and 0.868 (C).

Fig. 4. Mutual inhibition on OATP1B1-mediated uptake of [^{3}H]E$_2$G, [^{3}H]E$_1$S, and [^{3}H]BSP.

(A) concentration-dependent uptake of [^{3}H]E$_2$G (0.003 – 100 µM) for 5 min in the absence (closed circles) and presence of unlabeled E$_1$S (0.1 µM, open triangles) or BSP (0.3 µM, open squares). (B) concentration-dependent uptake of [^{3}H]E$_1$S (0.003 – 10 µM) for 1 min in the absence (closed circles) and presence of unlabeled E$_2$G (10 µM, open triangles) or BSP (0.3 µM, open squares). (C) concentration-dependent uptake of [^{3}H]BSP (0.007 – 10 µM) for 5 min in the absence (closed circles) and presence of unlabeled E$_2$G (10 µM, open triangles) or E$_1$S (10 µM, open squares). Data are shown as Eadie-Hofstee plots. Each point represents the mean ± SD (n=3). Fitted lines, which were obtained from nonlinear regression analysis based on the equation 3 or 4 under *Materials and Methods* are also presented. Representative data from three independent experiments are shown in this figure, and all individual data are given in Supplemental Fig. 1.

Table 1. IC$_{50}$ values for OATP1B1-mediated uptake of [^{3}H]E$_2$G, [^{3}H]E$_1$S, and [^{3}H]BSP

Inhibitors	Substrates		
	[^{3}H]E$_2$G	[^{3}H]E$_1$S	[^{3}H]BSP
	IC$_{50}$ (or K$_m$) µM		
E$_1$S	0.095 ± 0.015	0.271 ± 0.013[b]	0.429 ± 0.175[a]
			611 ± 387[a]
CsA	0.118 ± 0.015	0.732 ± 0.224	0.694 ± 0.149
BSP	0.131 ± 0.010	0.215 ± 0.058	0.327 ± 0.033[b]
ritonavir	0.397 ± 0.023	46.4 ± 9.8	3.38 ± 0.66
rifampin	0.585 ± 0.074	6.96 ± 1.31	2.75 ± 0.62
tacrolimus	0.668 ± 0.156	1.78 ± 0.34	3.57 ± 0.43
erythromycin	4.88 ± 0.65	13.4 ± 4.0	63.3 ± 11.5
E$_2$G	7.04 ± 0.53[b]	16.6 ± 2.4	39.3 ± 9.0
ketoconazole	9.90 ± 2.40	15.4 ± 3.7	60.9 ± 26.1
TCA	19.0 ± 1.0	50.0 ± 4.8	161 ± 35
verapamil	22.3 ± 4.2	44.0 ± 7.3	84.3 ± 30.1
gemfibrozil	26.4 ± 2.1	381 ± 60	173 ± 34
probenecid	79.4 ± 5.8	227 ± 69	740 ± 181

OATP1B1-mediated uptake of [^{3}H]E$_2$G (0.1 µM, 5 min), [^{3}H]E$_1$S (0.01 µM, 1 min), and [^{3}H]BSP (0.01 µM, 5 min) was examined in the presence and absence of inhibitors as shown in Fig. 2. IC$_{50}$ values were estimated by non-linear regression analysis based on equation 1 or 2 under *Materials and Methods*, and are presented as mean ± SD.
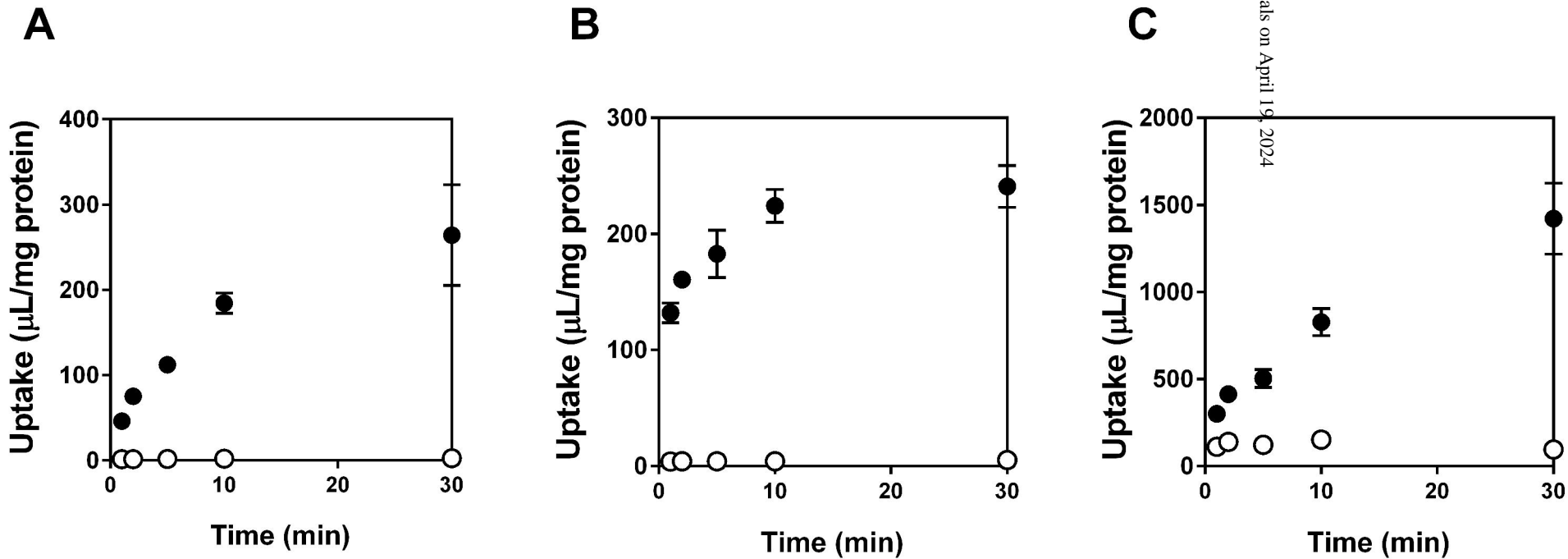
a: E$_1$S showed biphasic inhibition of [^{3}H]BSP uptake, and the IC$_{50}$ values for high and low affinity components are presented.

b: K$_m$ values.

29

Table 2. Saturation kinetics of OATP1B1-mediated uptake of [^{3}H]E$_2$G, [^{3}H]E$_1$S, and [^{3}H]BSP in the presence and absence of unlabeled E$_2$G, E$_1$S, and BSP

Inhibitor	Substrates						
	[^{3}H]E$_2$G[a]			[^{3}H]E$_1$S[b]		[^{3}H]BSP[c]	
	K$_m$	V$_{max}$	P$_{dif}$	K$_m$	V$_{max}$	K$_m$	V$_{max}$
	μM	pmol/min/mg	μL/min/mg	μM	pmol/min/mg	μM	pmol/min/mg
No inhibitor	8.17 ± 2.28	250 ± 89	NA	0.286 ± 0.054	36.4 ± 10.3	0.280 ± 0.041	20.8 ± 1.0
E$_2$G	NA	NA	NA	0.488 ± 0.072*	35.7 ± 8.3	0.361 ± 0.069	18.5 ± 1.9
E$_1$S	18.7 ± 2.2**	251 ± 22	NA	NA	NA	4.78 ± 0.65**	111 ± 18**
BSP	5.80 ± 2.53	55.8 ± 24.7**	0.667 ± 0.642	0.677 ± 0.112*	34.3 ± 11.7	NA	NA

Kinetic parameters were estimated by non-linear regression analysis based on the equation. 3 or 4 under *Materials and Methods*, and are shown as mean ± SD (n=3).

*$P < 0.05$ and **$P < 0.01$ compared to parameters determined without any inhibitors.

a: Concentration-dependent uptake of [^{3}H]E$_2$G (0.003 – 100 μM) for 5 min was examined in the absence and presence of unlabeled E$_1$S (0.1 μM) or BSP (0.3 μM).
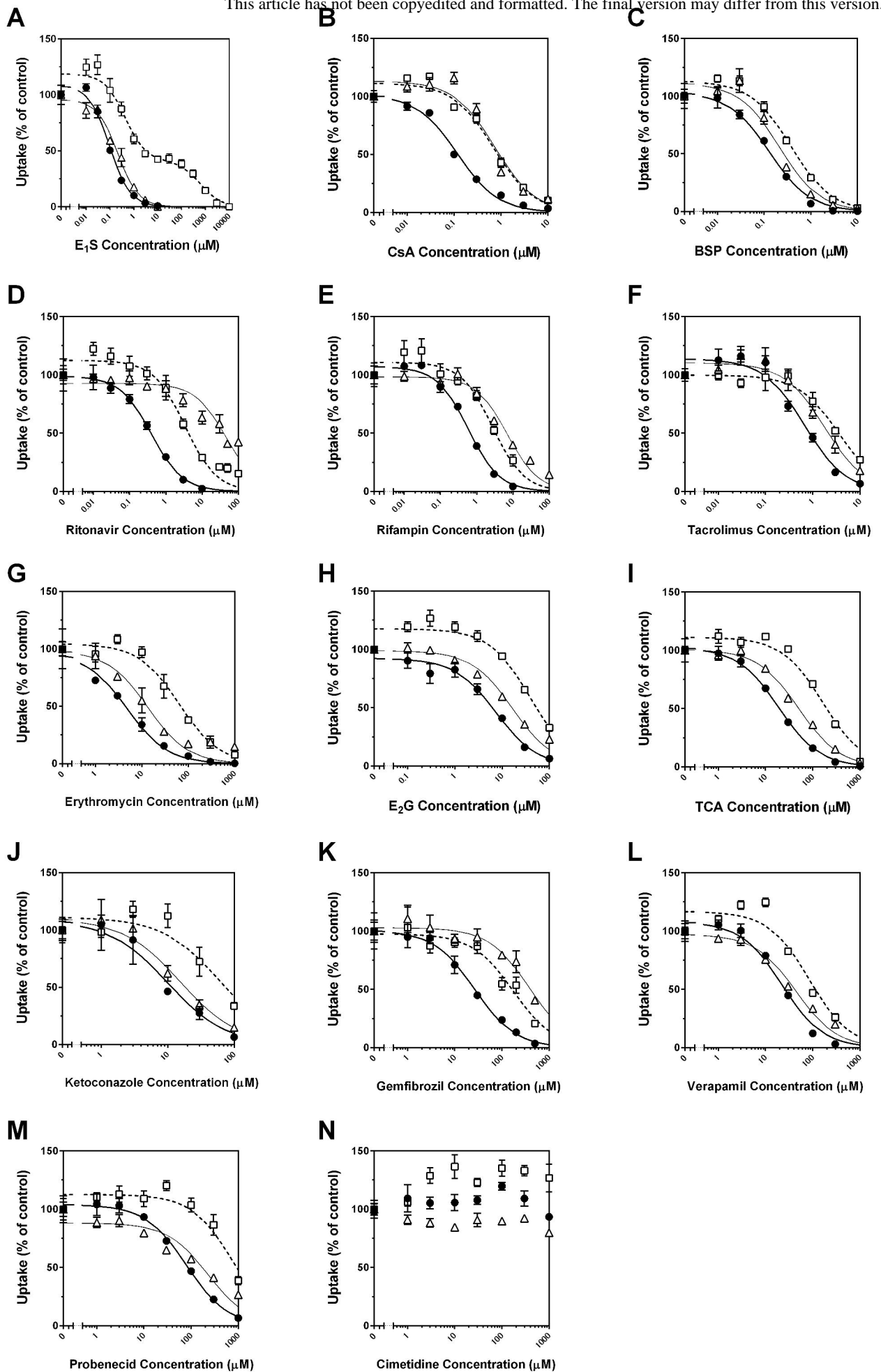
b: Concentration-dependent uptake of [^{3}H]E$_1$S (0.003 – 10 μM) for 1 min was examined in the absence and presence of unlabeled E$_2$G (10 μM) or BSP (0.3 μM).

c: Concentration-dependent uptake of [^{3}H]BSP (0.007 – 10 μM) for 5 min was examined in the absence and presence of unlabeled E$_2$G (10 μM) or E$_1$S (10 μM).
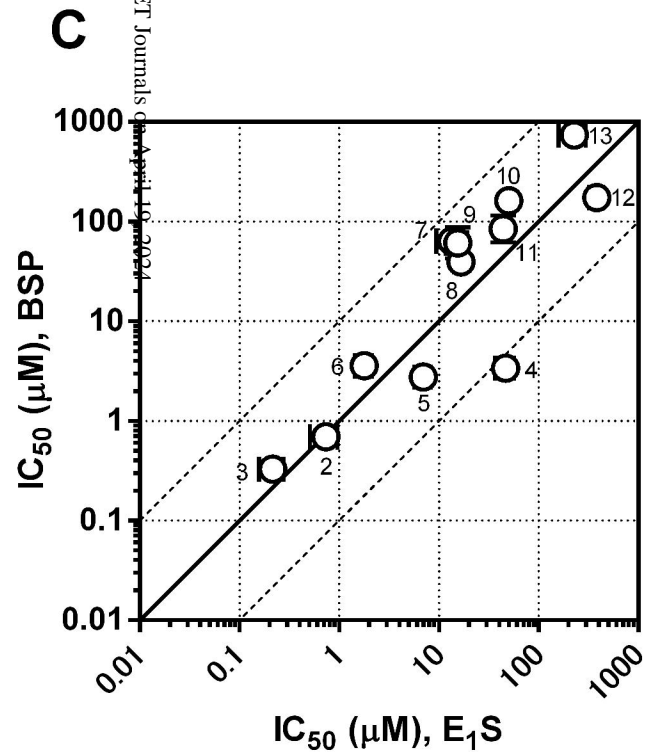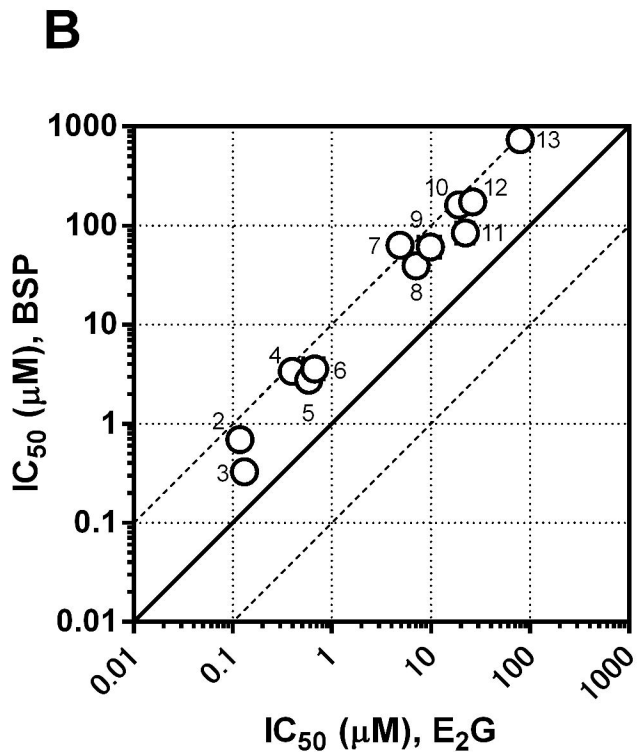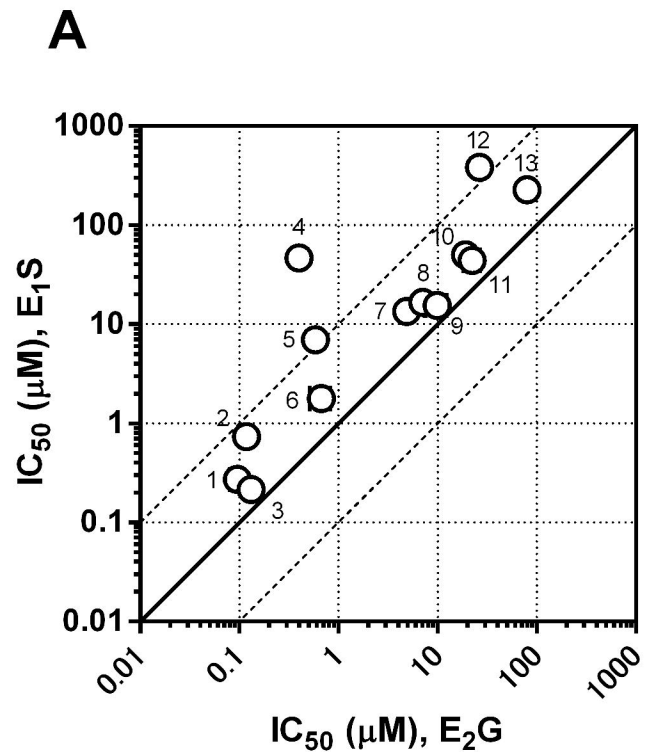
NA: Not applicable.

30

A

B

C

Figure 1

Figure 2

A

IC$_{50}$ (μM), E$_1$S vs IC$_{50}$ (μM), E$_2$G

B

IC$_{50}$ (μM), BSP vs IC$_{50}$ (μM), E$_2$G

C

IC$_{50}$ (μM), BSP vs IC$_{50}$ (μM), E$_1$S

Figure 3

Figure 4